Journal of Organometallic Chemistry 695 (2010) 2423–2431

Contents lists available at ScienceDirect

Journal of Organometallic Chemistry

journal homepage: www.elsevier.com/locate/jorganchem

Preparation of phosphinoferrocene carboxamides from isocyanates. Synthesis and structural characterisation of palladium(II) and platinum(II) complexes with 1′-(diphenylphosphino)-1-(*N*-phenylcarbamoyl)ferrocene

Petr Štěpnička*, Hana Solařová, Martin Lamač, Ivana Císařová

Department of Inorganic Chemistry, Faculty of Science, Charles University in Prague; Hlavova 2030, 12840 Prague, Czech Republic

ARTICLE INFO

Article history:
Received 21 April 2010
Received in revised form
13 July 2010
Accepted 15 July 2010
Available online 22 July 2010

Keywords:
Ferrocene
Carboxamides
Isocyanates
Palladium
Platinum
Structure elucidation

ABSTRACT

The reaction of *in situ* generated 1′-(diphenylphosphino)-1-lithioferrocene with isocyanates RNCO affords the respective phosphino-carboxamides $Ph_2PfcCONHR$ (fc = ferrocene-1,1′-diyl, R = cyclohexyl (**2**), and Ph (**3**)) in moderate yields. The coordination behaviour of **3** chosen as a representative was studied in palladium(II) and platinum(II) complexes. Depending on the metal precursor and the reaction conditions, the following compounds featuring this ligand as a P-monodentate or an *O*,*P*-chelating donor were isolated and characterised by spectroscopic methods (IR, multinuclear NMR and electrospray ionisation MS): *trans*-$[PdCl_2(\mathbf{3}\text{-}\kappa P)_2]$ (**5**), *trans*-$[PtCl_2(\mathbf{3}\text{-}\kappa P)_2]$ (**6**), *cis*-$[PtCl_2(\mathbf{3}\text{-}\kappa P)_2]$ (**7**), [*SP-4-4*]-$[(L^{NC})PdCl(\mathbf{3}\text{-}\kappa P)]$ (**8**; L^{NC} = 2-[(dimethylamino-κ*N*)methyl]phenyl-κC^1), and [*SP-4-3*]-$[(L^{NC})PdCl(\mathbf{3}\text{-}\kappa^2 O,P)]SbF_6$ (**9**). Besides, the crystal structures of a phosphine oxide resulting by oxidation of **2**, *viz* $Ph_2P(O)fcCONHCy$ (**4**), and of complexes $\mathbf{5}\cdot 2Et_2O$ and **9** have been determined by single-crystal X-ray diffraction analysis.

1. Introduction

Ferrocene-based phosphinocarboxamide donors were shown to be versatile ligands, finding applications in coordination chemistry and catalysis [1,2]. Most typically, these compounds are prepared via amide coupling of the respective phosphinocarboxylic acids and amines mediated by carbodiimide reagents [3] or, alternatively, by reactions of activated carboxylic derivatives (e.g., pentafluorophenyl esters) with amines [1i,4].

While looking for an alternative preparative route to ferrocene phosphino-carboxamides, isocyanates emerged as possible synthetic precursors. Indeed, the direct carbamoylation of ferrocene with isocyanates in the presence of $AlCl_3$ was reported already in 1957 [5]. However, this reaction proceeds under the usual Friedel–Crafts conditions, which could result in oxidation of the phosphine moiety and may thus lead to a lengthening of the synthesis route by the necessary protection/deprotection steps. A more promising route thus appeared to be the reaction of isocyanates with organometals as the nucleophiles. This reaction, although discovered as early as in 1901 [6], has found only surprisingly little use in ferrocene chemistry. The only example we are aware of is the synthesis of carboxamides from *ortho*-lithiated aminoferrocenes, [Fe{η^5-$C_5H_3((CH_2)_nNMe_2)$(CONHPh)-1,2}(η^5-C_5H_5)] ($n = 1$ and 2) [7]. A related approach, *not* making use of pre-formed metallocenes, was more recently utilised in the preparation of amide-substituted metallocenes via metathesis between metal halides and Li[C_5H_4C(O)NHR] salts, the latter being generated *in situ* from lithium cyclopentadienide and the respective isocyanate (R = *n*- and *t*-Bu, cyclohexyl, Ph, 3-pyridyl, and 2-tetrahydropyranyl) [8].

The relatively mild reaction conditions, generally good yields and simplicity of the direct reaction of the mentioned lithioferrocenes with isocyanates led us to extend this approach to 1′-(diphenylphosphino)-1-lithioferrocene. This reactive compound is readily prepared *in situ* via lithiation of stable 1′-(diphenylphosphino)-1-bromoferrocene and has already found manifold use in the preparation of 1′-functionalised ferrocene phosphines [9]. In this contribution, we demonstrate the validity of the 'isocyanate approach' outlined above, reporting on the preparation of two new ferrocene phosphine-carboxamides, $Ph_2PfcC(O)NHR$ (fc = ferrocene-1,1′-diyl; R = cyclohexyl (**2**), and Ph (**3**)). We also describe the synthesis and structural characterisation of some platinum(II) and palladium(II) complexes featuring compound **3** as a *P*-monodentate or an *O*,*P*-chelating donor.

* Corresponding author. Fax: +420 221 951 253.
E-mail address: stepnic@natur.cuni.cz (P. Štěpnička).

0022-328X/$ – see front matter © 2010 Elsevier B.V. All rights reserved.
doi:10.1016/j.jorganchem.2010.07.013

2. Results and discussion

2.1. Preparation and characterisation of phosphinoferrocene carboxamides

1′-(Diphenylphosphino)-1-lithioferrocene, generated conveniently *in situ* by lithiation of 1-bromo-1′-(diphenylphosphino) ferrocene (**1**) with *n*-butyllithium at low temperatures, reacts with cyclohexyl- or phenylisocyanate to give the corresponding phosphine-amides **2** and **3** (Scheme 1). Following the aqueous workup, the amides are isolated by column chromatography as analytically pure orange solids in moderate yields of 69% and 32%, respectively. It appears likely that the reaction is impeded by the solubility of the isocyanates in tetrahydrofuran at low temperatures. The reaction with the less soluble phenylisocyanate not only gives a lower yield of the 'coupling' product but also affords a relatively larger amount of (diphenylphoshino)ferrocene, resulting from protonolysis of the lithiated intermediate. Fortunately, however, this side-product is readily separated by column chromatography as a low-polar component. Another, more polar side-product, detected in the reaction leading to *N*-cyclohexyl amide **2**, was found to be the corresponding phosphine oxide **4** resulting in tiny amounts by accidental oxidation.

Compounds **2**–**4** were characterised by elemental analysis and by spectroscopic methods (multinuclear NMR, IR and mass spectra). In the NMR spectra, amides **2** and **3** display a set of characteristic virtual multiplets attributable to phosphorus-substituted ferrocene-1,1′-diyl unit and its PPh_2 and amide substituents. Resonances due to the amide protons (NH) of **2** and **3** are seen as a singlet (δ_H 7.75) or CH-coupled doublet (δ_H 5.78, $^3J_{HH} = 8.1$ Hz), respectively. ^{13}C NMR spectra of **2**–**4** support the formulation, showing signals of the 1′-(diphenylphosphino)ferrocene-1-yl moiety and the amide substituents. The resonances due to the amide C=O occur at δ_C ca. 168.5, which is similar to other Hdpf-based amides (Hdpf = 1′-(diphenylphosphino)ferrocene-1-carboxylic acid) [1a,b,e–j] and considerably upfield vs. free Hdpf [10].

The ^{31}P NMR signals of **2** and **3** are found at positions similar to Hdpf (δ_P −17.6 [10]). On the other hand, the oxidation of the phosphine groups in **4** is clearly manifested by a shift of the ^{31}P NMR resonance to lower fields (*cf.* δ_P +32.9 for HdpfO [10]) and further by shifts of the ^1H and ^{31}C signals and an increase in the J_{PC} coupling constants [11]. The presence of secondary amide groups is uniformly manifested via a broad ν_{NH} band at 3250–3300 cm^{-1}, and by amide I/II bands at ca. 1640/1530 cm^{-1} in the IR spectra.

Electrospray ionisation (ESI) mass spectra of **2** and **3** display dominant pseudomolecular ions ($[M + Na]^+$ or $[M - H]^-$), while the 'true' molecular ions ($M^{+\bullet}$) are seen in electron impact (EI) mass spectra. The EI mass spectra of **2** and **3** further show ions resulting by simple fragmentation $[M - R]^+$ (*m*/*z* 412, R = Cy or Ph), $[M - NHR]^+$ (*m*/*z* 397 [12]), and $[M - C_5H_4CONHR]^+$ (*m*/*z* 305), and fragments typical for the EI-induced decomposition of the (diphenylphosphino)ferrocene unit (*m*/*z* 226/227, 197, 170/171, 141) [13] and the PPh_2 group (*m*/*z* 183, $[Ph_2P - 2H]^+$). The presence of fragment ions,

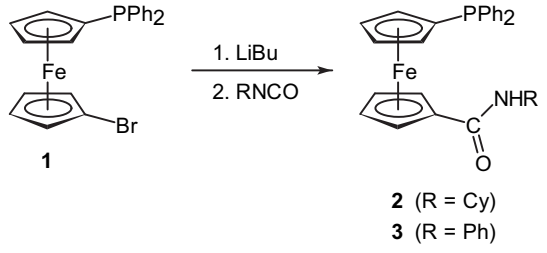

Scheme 1. Preparation of amidophosphine ligands **2** and **3**.

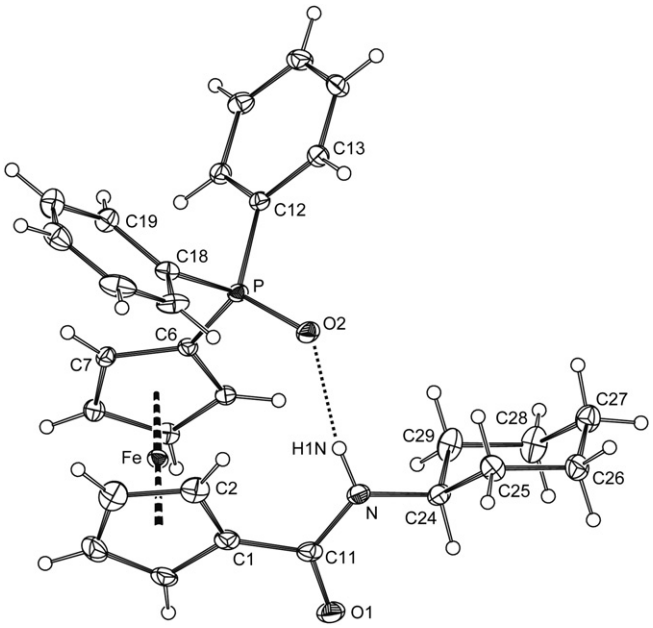

Fig. 1. A view of the molecular structure of **4** showing the atom labelling scheme and displacement ellipsoids at 30% probability level. The intramolecular N–H···O hydrogen bond is indicated with a dotted line.

which can be tentatively formulated as $[FcPPh_2O]^{+\bullet}$ (*m*/*z* 386), $[FcPPh_2O - C_5H_5]^+$ (*m*/*z* 321; intense signals) and $[Ph_2PO]^+$ (*m*/*z* 201), suggests that the decomposition of $\mathbf{2}^{+\bullet}$ and $\mathbf{3}^{+\bullet}$ involves a transfer of oxygen atom from the amide group to phosphorus as previously observed for Hdpf and the related compounds [13].

2.2. The crystal structure of 4

In addition to spectroscopic characterisation, the crystal structure of **4** was determined by single-crystal X-ray diffraction analysis. A view of the molecular structure is shown in Fig. 1. Selected geometric data are given in Table 1.

Compound **4** crystallises with the symmetry of the monoclinic space group $P2_1/n$ and one molecule in the asymmetric unit. Because the amide NH proton as the only conventional hydrogen bonding acceptor is saturated by *intra*molecular P=O···H–N hydrogen bond, the individual molecules in the crystal associate only via soft interactions. These include mainly *inter*molecular

Table 1
Selected distances and angles for **4** (in Å and °).[a]

Fe–Cg1	1.649(1)	∠Cp1,Cp2	1.0(1)
Fe–Cg2	1.642(1)	τ[b]	77
C1–C11	1.488(3)	ψ[c]	24.6(3)
C11–O1	1.234(3)	O1–C11–N	123.1(2)
C11–N	1.347(3)	C11–N–C24	121.7(2)
N–C24	1.459(3)	O1–C11–N–C24	172.7(2)
P–O2	1.490(2)	O2–P–C[d]	112.48(9)–113.59(9)
P–C6	1.786(2)	C–P–C[e]	104.85(9)–105.89(9)
P–C12	1.806(2)	φ[f]	0.0(3)
P–C18	1.807(2)	Q[f]	0.567(3)

[a] Definition of the ring planes: Cp1 = C(1–5), Cp2 = C(6–10); Cg1 and Cg2 are the respective ring centroids.
[b] Torsion angle C1–Cg1–Cg2–C6.
[c] Dihedral angle of the Cp1 and {C11,O1,N} planes.
[d] The range of O2–P–C(6,12,18) angles.
[e] The range of C6–P–C(12,18) and C12–P–C18 angles.
[f] Ring puckering parameters for the cyclohexyl group C(24–29) (Q = total puckering amplitude; ideal chair requires φ = 0°).

C–H···O hydrogen bonds involving the aromatic CH groups and P=O or C=O oxygens (Table 2), and supportive C–H···π-ring interactions (C9–H9···Ph1^{i}: C9···Cg(Ph1^{i}) = 3.706(2) Å, C9–H9···Cg(Ph1^{i}) = 160°; C14–H14···Ph2^{ii}: C14···Cg(Ph2^{ii}) = 3.525(2) Å, C14–H14···Cg(Ph2^{ii}) = 169°; Ph1 = C(12–18), Ph2 = C(18–23), Cg denotes the ring centroids; i = 1/2 − *x*, 1/2 + *y*, 1/2 − *z*, ii = 1 − *x*, −*y*, 1 − *z*).

The molecular geometry of the phosphine oxide is unexceptional. The parameters of the amide moiety are similar to other Hdpf-based amides [1b,d,f,h–j] while the P=O bond length is identical to that observed for crystalline HdpfO (1.487(2) Å at 23 °C [10]). The ferrocene cyclopentadienyls in **4** are tilted negligibly (tilt angle ca. 1°) and assume a conformation near to synclinal eclipsed (ideal value: $\tau = 72°$). Such conformation and the observed rotation of the amide moiety along the pivotal C1–C11 bond (see ψ angle in Table 1) apparently facilitate the formation of the intramolecular N–H···O=P hydrogen bond. The pendant cyclohexyl group adopts a chair conformation (see the ring puckering parameters [14] in Table 2) and binds to the amide nitrogen atom in an equatorial position.

2.3. Preparation of complexes from ligand *3*

The reactions of amidophosphine **3** (two molar equivalents) with [$PdCl_2$(cod)] (cod = η^2:η^2-cycloocta-1,5-diene) or $K_2[PtCl_4]$ gave rise to the expected *trans*-bis(phosphine) complexes, *trans*-[MCl_2(**3**-κ*P*)$_2$] (**5**, M = Pd; **6**, M = Pt; Scheme 2). A similar reaction with [$PtCl_2$(cod)] afforded the isomeric compound, *cis*-[$PtCl_2$(**3**-κ*P*)$_2$] (**7**). The complexes were isolated as air stable solids with a strong tendency to hold the reaction solvents. They were characterised by ^{1}H and ^{31}P NMR spectra, IR and ESI mass spectra, and by elemental analysis.

ESI mass spectra corroborate the formulation of **5**–**7** by showing ions due to $[M + Na]^+$ (for **5** and **6**), $[M - Cl]^+$ (for **5** and **7**), or deprotonated molecular ions $[M - H]^-$ (for **6** and **7**). The ^{1}H NMR spectra of **5**–**7** display one set of resonances due to coordinated **3**, thereby suggesting equivalency of the metal-bound ligands. Signals in the ^{31}P NMR spectra of the complexes are found shifted to lower fields as compared to free **3**. For the platinum complexes, the ^{31}P NMR resonances are flanked with ^{195}Pt satellites with characteristic coupling constants (**6**: $^1J_{PtP}$ = 2604 Hz; **7**: $^1J_{PtP}$ = 3786 Hz) [15]. The ^{31}P NMR parameters of **5**–**7** compare well with those of the analogous complexes [MCl_2(Hdpf-κ*P*)$_2$] [16] and thus indicate P-monodentate coordination of **3** for all complexes. Indeed, this is in line with the IR spectra confirming the amide group to remain uncoordinated.

Table 2
Hydrogen bond parameters for **4**, **5**·2Et_2O and **9** (in Å and °).

D–H···A	D···A	Angle at H
Compound **4**		
N–H···O2	3.012(2)	171
C8–H8···O2^{i}	3.462(3)	162
C16–H16···O1^{ii}	3.396(3)	157
Compound **5**·2Et_2O		
N–H1N···O^{iii}	3.129(4)	166
C2–H2···O^{iii}	3.401(5)	156
C27–H27···O^{iii}	3.281(6)	136
Compound **9**		
N1–H1N···F6^{iv}	3.062(4)	162
C2–H2···F6^{iv}	3.237(5)	158
C28–H28···F3^{vi}	3.156(6)	139
C37–H37A···F2	3.449(6)	159

D = donor, A = acceptor. Symmetry operations: i −1/2 + *x*, 1/2 − *y*, −1/2 + *z*; ii = 1/2 − *x*, −1/2 + *y*, 1/2 − *z*; iii = *x*, 1/2 − *y*, 1/2 + *z*; iv = *x*, 1/2 − *y*, 1/2 + *z*; vi = −*x*, 1 − *y*, 1 − *z*.

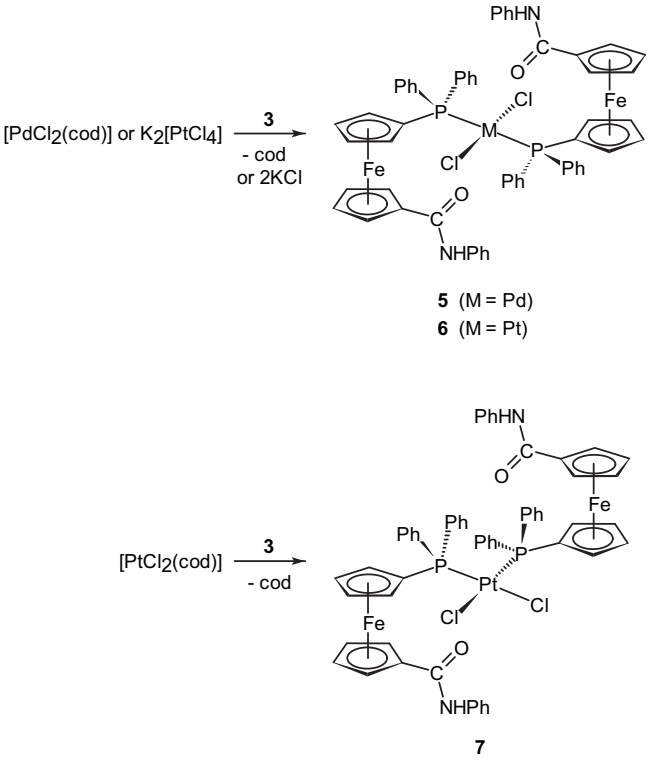

Scheme 2. Preparation of bis(phosphine) palladium(II) and platinum(II) complexes.

A reaction between stoichiometric amounts of **3** and dimer [(L^{NC})PdCl]$_2$ (L^{NC} = [2-(dimethylamino-κ*N*)methyl]phenyl-κC^1) produced the bridge-cleavage product featuring donor **3** as a simple phosphine, [(L^{NC})PdCl(**3**-κ*P*)] (**8**; Scheme 3). Upon removal of the chloride ligand from **8** with silver(I) hexafluoroantimonate, the ferrocene ligand takes up the liberated coordination site while **8** is

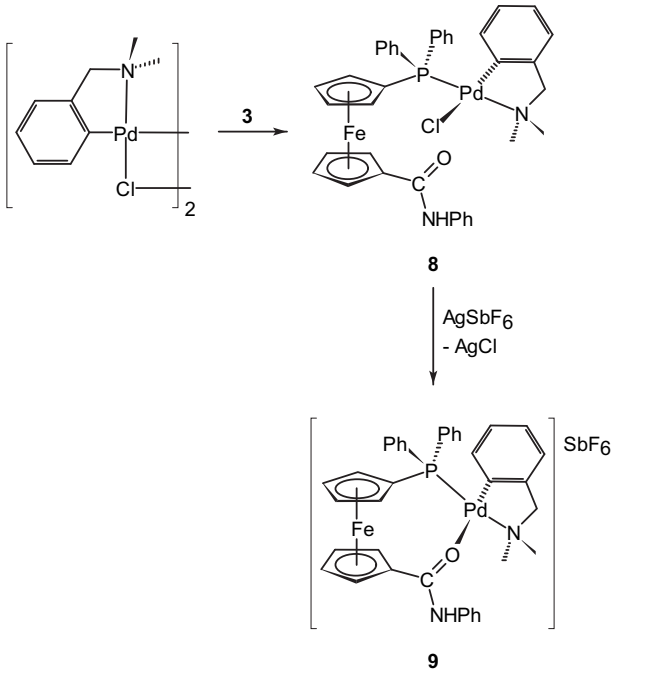

Scheme 3. Preparation of palladium(II) complexes with auxiliary 2-[(dimethylamino)methyl]phenyl ligand.

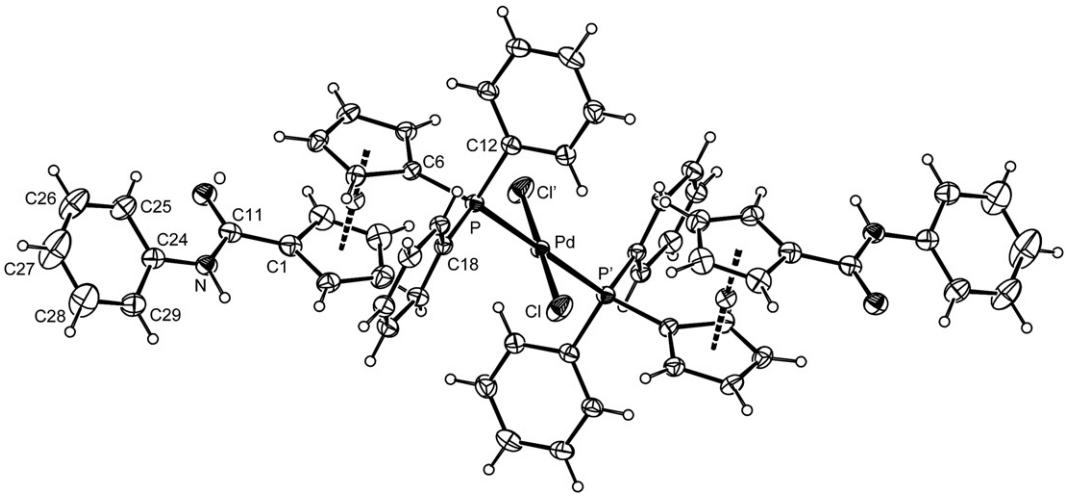

Fig. 2. A view of the complex molecule in the structure of **5**·2Et$_2$O showing atomic labels and displacement ellipsoids at 30% probability level.

smoothly converted into a cationic bis-chelate complex [(L^{NC})PdCl(**3**-κ^2*O*,*P*)] (**9**).

The ^{1}H NMR spectra of **8** and **9** combine characteristic signals due to ligand **3** and the Pd-bound $C_6H_4CH_2NMe_2$ moiety. The P-coordination of the amidophosphine ligand is manifested by the shift of the ^{31}P NMR resonance to lower fields (coordination shifts; **8**: $\Delta_P = 49.6$; **9**: $\Delta_P = 47.7$ ppm) and the coupling of the NCH_2 and NMe_2 protons with phosphorus (the $^4J_{PH}$ constants) [17] suggest *trans*-P–N relationship in both cases. Positive-ion ESI mass spectra of **8** and **9** are dominated by the ions $[(L^{NC})Pd(\mathbf{3})]^+$ at *m*/*z* 729 (*i.e.*, $[M - Cl]^+$ for **8**). On the other hand, the spectra recorded in negative ion mode either confirm the formulation (ions due to $[M - H]^-$ and $[L - H]^-$ are seen for **8**) or indicate the presence of the counter ion (**9**: *m*/*z* 235/237). The presence of SbF_6^- is further reflected in IR spectra showing a strong and structured band at ca. 660 cm^{-1} [18]. Besides, the IR spectra clearly indicate the involvement of the amide C=O group in coordination. Whereas complex **8** featuring P-monodentate **3** shows amide I band (largely $\nu_{C=O}$) at 1666 cm^{-1}, the cationic bis-chelate **9** has the same band shifted by 55 cm^{-1} to lower energies (1611 cm^{-1}).

2.4. The crystal structures of **5**·2Et$_2$O and **9**

A careful recrystallisation of **5** from chloroform/diethyl ether afforded the crystalline solvate **5**·2Et$_2$O [19]. The solvent molecules in the structure of **5**·2Et$_2$O were found to be severely disordered in structural voids defined by the bulky complex molecules and, therefore, their contribution was numerically subtracted from the overall scattering (see Experimental). A view of the complex molecule is presented in Fig. 2. Pertinent geometric parameters are summarised in Table 3.

The complex crystallises with the symmetry of the monoclic space group $P2_1/c$ having its palladium atom located on the crystallographic inversion centre. As a result, the coordination sphere is ideally planar though with the interligand angles differing slightly from the ideal 90°. The Pd-donor distances are similar to those reported for *trans*-[PdCl$_2$(Hdpf-κ*P*)$_2$]·2CH$_3$CO$_2$H [16]. The uncoordinated amide moiety is tilted with respect to its parent cyclopentadienyl ring (see ψ angle in Table 3) and, mainly, rotated away from the coordinated metal ($\tau = 145°$). This brings the amide units to less sterically encumbered areas and allows them to form N–H···O=C hydrogen bonds with the proximal ligand moieties (Table 2). Interestingly, the N–H···O interaction is supported via cooperative soft C–H···O contacts from the ferrocene H2 and the phenyl H29 that are both adjacent to the amide moiety and directed towards the same carbonyl oxygen (Fig. 3a). Since each complex molecule has two amide units and the H-bond contacts involve ligands from different complex molecules (not related by simple translation), the hydrogen bond interactions result in the formation of infinite, sheet-like assemblies oriented parallel to the crystallographic *bc* plane (Fig. 3b).

A view of the molecular structure of the cation in the structure of complex **9** is shown in Fig. 4. Selected geometric data are given in Table 4. The overall geometry of the cation compares well with that observed for an analogous complex featuring a related functional amide as an *O*,*P*-chelating donor, [(L^{NC})Pd(Ph$_2$*P*fc*CO*NHCH$_2$CO$_2$Me)]ClO$_4$ [1h]. Similarly to this reference compound, the coordination environment of the palladium atom is angularly distorted owing to unlike steric demands of the chelating ligands: The N2–Pd–C30 angle within the small metallacycle is expectedly the most acute, while the O–Pd–P angle associated with the chelating ferrocene ligand is the most opened. The atoms constituting the coordination plane (Pd,P,O,N2,C30) are coplanar within ca. 0.15 Å. The {(L^{NC})Pd} ring assumes an envelope conformation with N2 projecting by ca. 0.3 Å from the plane of the remaining atoms.

The ferrocene unit in **9** shows a tilt of ca. 5° and an insignificant variation in the Fe–Cg distances (the individual Fe–C distances

Table 3
Selected distances and angles for **5**·2Et$_2$O (in Å and °).[a]

Pd–Cl	2.284(1)	Cl–Pd–P[b]	87.97(4)
Pd–P	2.3310(8)	∠PdL$_4$,Cp2	35.2(2)
Fe–Cg1	1.647(2)	∠Cp1,Cp2	1.9(2)
Fe–Cg2	1.652(2)	τ[c]	145
C1–C11	1.483(6)	ψ[d]	7.5(5)
C11–O	1.227(4)	O–C11–N	123.4(4)
C11–N	1.357(5)	C11–N–C24	128.1(3)
N–C24	1.409(5)	∠Cp1,Ph^N	32.9(3)
P–C6	1.797(3)	O–C11–N–C24	8.5(7)
P–C12	1.819(4)	Pd–P–C[e]	107.5(1)–122.0(1)
P–C18	1.829(3)	C–P–C[f]	100.0(2)–105.5(2)

[a] Definition of the ring planes: Cp1 = C(1–5), Cp2 = C(6–10), PdL4 = {Pd,Cl,Cl′,P,P′}, Ph^N = C(24–29). The primed atoms are generated by the crystallographic inversion operation. Cg1 and Cg2 denote centroids of the rings Cp1 and Cp2, respectively.
[b] The Cl–Pd–P and Cl–Pd–P′ angles sum to exactly 180° due to imposed symmetry.
[c] Torsion angle C1–Cg1–Cg2–C6.
[d] Dihedral angle of the Cp1 and {C11,O,N} planes.
[e] The range of Pd–P–C(6,12,18) angles.
[f] The range of C6–P–C(12,18) and C12–P–C18 angles.

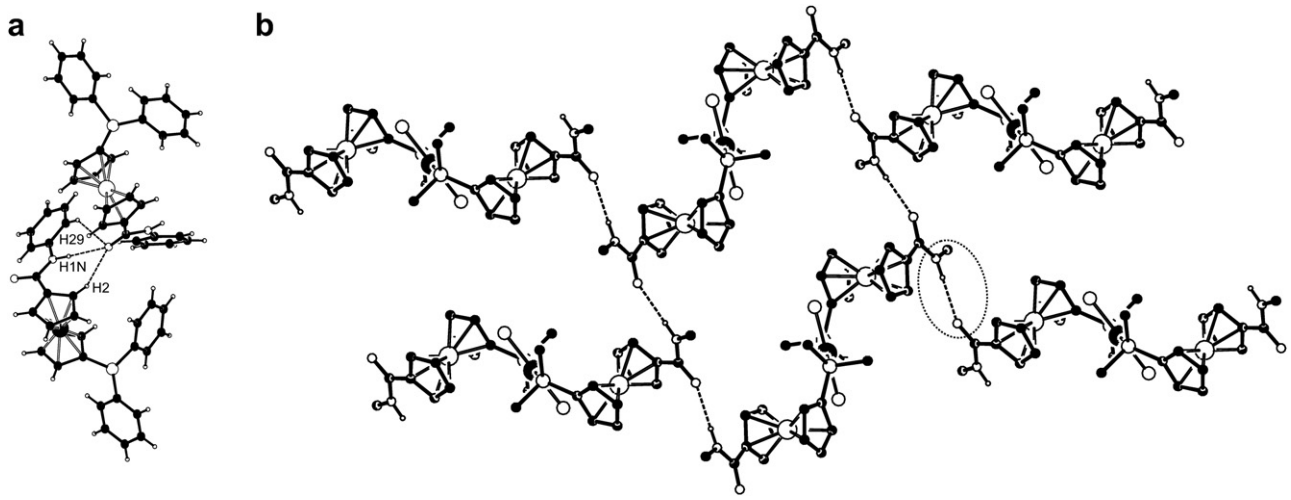

Fig. 3. (a) A view of the basic hydrogen-bonded unit in the structure of **5**·2Et$_2$O showing the cooperative N–H···O and C–H···O hydrogen bonds as dashed lines. (b) Section of the hydrogen-bonded array in the same crystal structure. For clarity, only the pivotal phenyl ring carbons and relevant hydrogen atoms are shown and the supportive C–H···O contacts are omitted.

range 2.001(4)–2.074(4) Å). More importantly, the ferrocene substituents are rotated to an intermediate conformation between synclinal staggered ($\tau = 36°$) and synclinal eclipsed ($\tau = 72°$), which enables their simultaneous coordination. Likewise, the amide moiety (C11,N1,O) is rotated along its pivotal C1–C11 bond (see ψ angle in Table 4) and, simultaneously, bent towards the palladium with the dihedral angle of the C1–C11 bond and the Cp1 plane being 9.6(3)° (*N.B.* The dihedral angle subtended by the P–C6 bond and the Cp2 plane is only 1.2(2)°). The coordinated C=O bond is by ca. 0.14 Å longer than in **4**.

The geometry of the compensating SbF_6^- anion is rather unexceptional (Sb–F 1.858(3)–1.885(3) Å, F–Sb–F angles 88.2(1)–91.2 (1)°). In the solid state, however, the anions interact with the proximal complex cations via N–H···F and C–H···F hydrogen bonds (Fig. 5 and Table 2).

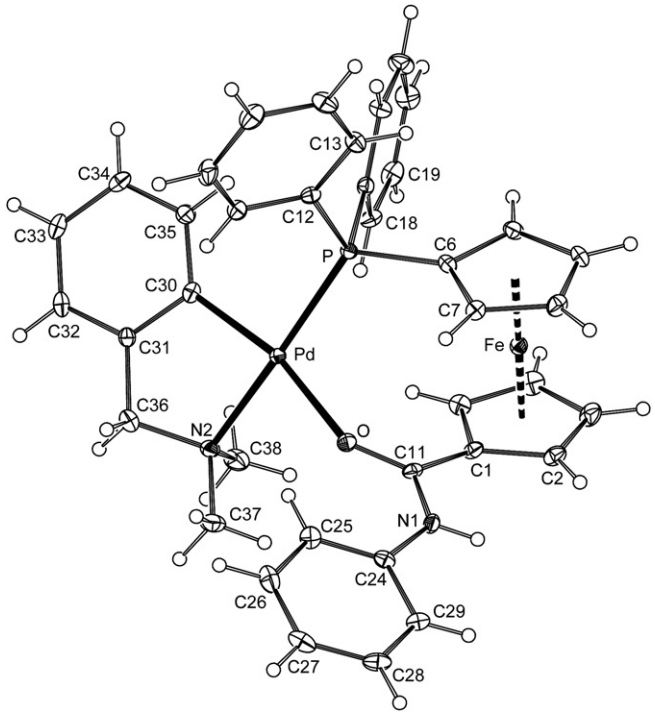

Fig. 4. A view of the molecular structure of **9** showing the atom labelling scheme and displacement ellipsoids at 30% probability level.

Table 4
Selected distances and angles for **9** (in Å and °).[a]

Pd–P	2.273(1)	P–Pd–O	99.02(8)
Pd–O	2.156(3)	P–Pd–C30	92.9(1)
Pd–N2	2.143(3)	N2–Pd–O	86.4(1)
Pd–C30	2.011(4)	N2–Pd–C30	82.6(1)
Fe–Cg1	1.640(2)	∠PdL$_4$,Cp2	53.5(2)
Fe–Cg2	1.627(2)	∠Cp1,Cp2	4.7(2)
C11–O	1.248(5)	τ[b]	62
C11–N	1.349(5)	O–C11–N1	121.0(4)
C1–C11	1.458(6)	ψ[c]	19.0(4)
N1–C24	1.422(5)	Pd–P–C[d]	113.9(1)–118.8(1)
P–C	1.802(4)–1.826(4)	C–P–C[e]	98.1(2)–108.4(2)

[a] Definition of the ring planes: Cp1 = C(1–5), Cp2 = C(6–10), PdL4 = {Pd,P,O,N2,C30}. Cg1 and Cg2 are centroids of the rings Cp1 and Cp2, respectively.
[b] Torsion angle C1–Cg1–Cg2–C6.
[c] Dihedral angle of the Cp1 and {C11,O,N} planes.
[d] The range of Pd–P–C(6,12,18) angles.
[e] The range of C6–P–C(12,18) and C12–P–C18 angles.

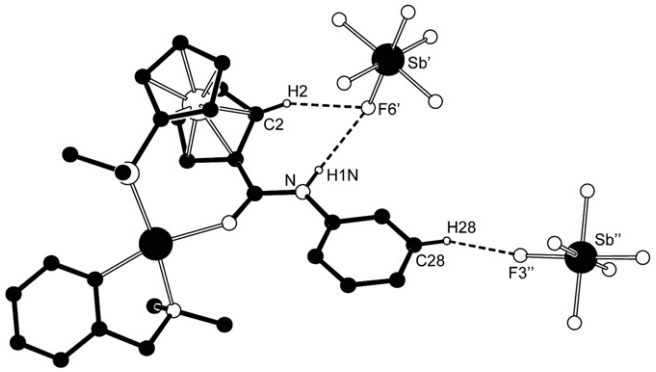

Fig. 5. The C–H···F contacts operating in the crystals of complex **9**. For clarity, only the relevant hydrogen atoms and pivotal carbons from the PPh$_2$ moiety are shown. The prime- and double prime-labelled atoms are generated by the (x, 1/2 − y, 1/2 + z) and (−x, 1 − y, 1 − z) symmetry operations, respectively. Some additional interactions, absent in this figure, are discussed in the text.

Table 5
Selected crystallographic data, data collection and structure refinement parameters for **4**, **5**·2Et$_2$O and **9**.

Compound	**4**	**5**·2Et$_2$O	**9**
Formula	$C_{29}H_{30}FeNO_2P$	$C_{66}H_{68}Cl_2Fe_2N_2O_4P_2Pd$[e]	$C_{38}H_{36}F_6FeN_2OPPdSb$[f]
M [g mol^{-1}]	511.36	1304.16	965.66
Crystal system	Monoclinic	Monoclinic	Monoclinic
Space group	$P2_1/n$ (no. 14)	$P2_1/c$ (no. 14)	$P2_1/c$ (no. 14)
T [K]	150(2)	150(2)	150(2)
a [Å]	12.4534(2)	11.6197(2)	19.257(2)
b [Å]	12.9372(2)	24.6950(8)	10.7485(5)
c [Å]	16.2744(3)	10.5699(3)	17.142(2)
β [°]	110.463(1)	101.027(2)	95.930(7)
V [Å^3]	2456.55(7)	2977.0(1)	3529.1(6)
Z	4	2	4
D_{calc} [g mL^{-1}]	1.383	1.455	1.817
μ(MoKα) [mm^{-1}]	0.706	0.973	1.782
T-range[a]	0.424–0.836	0.740–0.878	0.676–0.823
Diffractions total	37579	24129	31872
R_{int} [%][b]	6.06	4.19	11.13
Unique diffractions	5634	6782	7986
Observed[c] diffractions	4830	5288	5796
R (obsd diffrns) [%][c,d]	4.01	5.12	4.12
R, wR (all diffrns) [%][d]	4.89, 10.97	6.65, 15.13	7.62, 8.39
$\Delta\rho$ [e Å^{-3}]	1.90, −0.46	3.23, −1.40	0.79, −1.17
CCDC entry	773800	773801	773802

[a] The range of absorption coefficients.
[b] $R_{int} = \Sigma|F_o^2 - F_o^2(\text{mean})|/\Sigma F_o^2$, where F_o^2(mean) is the average intensity of symmetry-equivalent diffractions.
[c] Diffractions with $I_o > 2\sigma(I_o)$.
[d] $R = \Sigma||F_o| - |F_c||/\Sigma|F_o|$, $wR = [\Sigma\{w(F_o^2 - F_c^2)_2\}/\Sigma w(F_o^2)^2]^{1/2}$.
[e] $C_{58}H_{48}Cl_2Fe_2N_2O_2P_2Pd \cdot 2C_4H_{10}O$ (see Experimental).
[f] $[C_{38}H_{36}FeN_2OPPd]SbF_6$.

3. Conclusion

As evidenced by the preparation of two new phosphinoferrocene carboxamides **2** and **3**, the reaction of substituted lithioferrocenes with isocyanates represents a viable route to functional ferrocene carboxamides. Compared to carbodiimide-mediated amide coupling method, which is frequently used in the synthesis of ferrocene carboxamides, a wide implementation of this methodology could be hindered by the availability and properties (solubility) of the required isocyanates. However, its use seems to be warranted for amines (*e.g.*, aromatic), which are difficult to couple under conventional conditions.

The coordination study performed with ligand **3** and platinum and palladium as the metals expectedly demonstrated that this phosphine-amide binds to these soft metals preferentially via its soft phosphorus donor atom while the carbamoyl unit remains uncoordinated and takes part in intermolecular interactions. Yet, a P,O-chelate coordination of the *same* ligand can be readily imparted after creating a free coordination site at the central atom, *e.g.*, via removal of an auxiliary ligand.

4. Experimental

4.1. Materials and methods

Syntheses were performed under an argon atmosphere. Tetrahydrofuran was distilled from potassium/benzophenone ketyl. Dichloromethane and chloroform were dried over anhydrous K_2CO_3 and distilled afterwards. 1′-(Diphenylphosphino)-1-bromoferrocene (**1**) [9a], [MCl_2(cod)] (M = Pd or Pt) [20], and [{(L^{NC})PdCl}$_2$] (L^{NC} = [2-(dimethylamino-κ*N*)methyl]phenyl-κ*C*^{1}) [21] were prepared by literature methods. Other chemicals and solvents were used as received from commercial sources.

NMR spectra were measured on a Varian Unity Inova 400 spectrometer (^{1}H, 399.95; ^{13}C, 100.58; ^{31}P, 161.90 MHz) at 25 °C. Chemical shifts (δ/ppm) are given relative to internal $SiMe_4$ (^{13}C and ^{1}H) or to external 85% aqueous H_3PO_4 (^{31}P). Infrared spectra were recorded with a Nicolet 7600 (Thermo Fisher Scientific) spectrometer in the range 400–4000 cm^{-1}. Positive-ion electron impact (EI$^+$) mass spectra including the high resolution (HR) data were obtained with a GCT premier spectrometer (Waters). Electrospray (ESI) mass spectra were recorded with a Bruker Esquire 3000 spectrometer. The samples were dissolved in dichloromethane and diluted with methanol in excess.

4.2. Preparation of 1′-(diphenylphosphino)-1-(*N*-cyclohexylcarbamoyl)ferrocene (**2**)

n-Butyllithium (0.5 mL 2.5 M in hexanes, 1.3 mmol) was added slowly to a solution of bromide **1** (450 mg, 1.0 mmol) in dry tetrahydrofuran (20 mL) while cooling to ca. −78 °C (dry ice/ethanol bath). After stirring at this temperature for 50 min, neat cyclohexyl isocyanate (150 mg, 1.2 mmol) was introduced and stirring was continued overnight at room temperature. The resultant orange-brown mixture was quenched with water and brine (10 mL each) and extracted with diethyl ether (2 × 30 mL). Combined organic layers were dried over $MgSO_4$ and evaporated under vacuum. The residue was purified by chromatography on a silica gel column using dichloromethane/methanol (50:1 v/v) as the eluent. The first band containing only (diphenylphosphino)ferrocene was discarded and the following one containing the desired amide was collected and evaporated under vacuum. Yield of **2**: 334 mg (69%), orange solid.

Prolonged elution (with the same solvent mixture) led to the development of an additional minor orange band due to phosphine oxide **4**. This band was also collected and evaporated to afford crude **4**, which was subsequently crystallised from ethyl acetate/hexane at 4 °C. The separated crystals were filtered off, washed successively with ethyl acetate/hexane (1:1 v/v) and pentane, and dried under vacuum. Yield of **4**: 9 mg (2%), orange brown crystalline solid.

4.2.1. Analytical data for **2**

^{1}H NMR ($CDCl_3$): δ 1.04–2.00 (m, 10H, CH_2 of C_6H_{11}), 3.84–3.93 (m, 1H, CH of C_6H_{11}), 4.04 (vt, J' = 1.8 Hz, 2H, fc), 4.18 (vt, J' = 1.9 Hz,

2H, fc), 4.40 (vt, $J' = 1.8$ Hz, 2H, fc), 4.54 (vt, $J' = 1.9$ Hz, 2H, fc), 5.78 (d, $^3J_{HH} = 8.1$ Hz, 1H, NH), 7.31–7.40 (m, 10H, PPh_2). $^{31}P\{^1H\}$ NMR ($CDCl_3$): δ −16.9 (s). $^{13}C\{^1H\}$ NMR ($CDCl_3$): δ 24.93 (s, 2 C, CH_2 of C_6H_{11}), 25.61 (s, 1C, CH_2 of C_6H_{11}), 33.47 (s, 2C, CH_2 of C_6H_{11}), 48.25 (s, 1C, CH of C_6H_{11}) 69.56 (s, 2C, CH of fc), 71.35 (s, 2C, CH of fc), 72.86 (d, $J_{PC} = 4$ Hz, 2C, CH of fc), 74.42 (d, $J_{PC} = 15$ Hz, 2C, CH of fc), 128.27 (d, $^3J_{PC} = 6$ Hz, 4C, CH_m of PPh_2), 128.75 (s, 2C, CH_p of PPh_2), 133.44 (d, $^2J_{PC} = 20$ Hz, 4C, CH_o of PPh_2), 138.34 (d, $^1J_{PC} = 9$ Hz, 2C, C_{ipso} of PPh_2), 168.71 (s, 1C, C═O); signals due to C_{ipso}(fc) are probably obscured by the solvent resonance. IR (neat): ν 3320 br s, 3069 m, 3052 m, 2931 s, 2853 s, 1699 m, 1629 s, 1541 s, 1478 w, 1451 w, 1434 m, 1380 m, 1319 m, 1181 m, 1161 m, 1027 s, 891 m, 832 s, 820 m, 747 s, 697 s, 495 s, 453 w cm^{-1}. ESI ± MS: *m/z* 495/496 (M^+/$[M + H]^+$), 518 ($[M + Na]^+$), 534 ($[M + K]^+$); 494 ($[M - H]^-$). EI^+ MS: *m/z* (relative abundance) 497 (6), 496 (44), 495 (76, $M^{+\bullet}$), 494 (6), 493 (10), 414 (6), 413 (44), 412 (84, $[M - Cy]^+$), 410 (8), 401 (18), 400 (83), 399 (25), 398 (8), 397 (7), 386 (11), 370 (4), 322 (33), 321 (100, $[C_5H_4PPh_2FeO]^+$), 320 (6), 319 (12), 305 (12, $[C_5H_4PPh_2Fe]^+$), 304 (5), 303 (12), 295 (12), 294 (74), 229 (4), 227 (7), 226 (16), 202 (13), 201 (89, $[Ph_2PO]^+$), 197 (11), 183 (11, $[PPh_2 - 2H]^+$), 171 (21), 170 (17), 121 (9). HR MS calc. for $C_{29}H_{30}{}^{56}FeNOP$ ($M^{+\bullet}$) 495.1414, found 495.1409.

4.2.2. Analytical data for **4**

^1H NMR ($CDCl_3$): δ 1.21–2.03 (m, 10H, CH_2 of C_6H_{11}), 3.87–3.95 (m, 1H, CH of C_6H_{11}), 4.11 (vq, $J' = 1.9$ Hz, 2H, fc), 4.20 (vt, $J' = 2.0$ Hz, 2H, fc), 4.60 (vq, $J' = 1.8$ Hz, 2H, fc), 5.12 (vt, $J' = 1.9$ Hz, 2H, fc), 7.51–7.80 (m, 10H, PPh_2), 8.62 (d, $^3J_{HH} = 8$ Hz, 1H, NH). $^{31}P\{^1H\}$ NMR ($CDCl_3$): δ +30.6 (s). $^{13}C\{^1H\}$ NMR ($CDCl_3$): δ 25.36 (s, 2C, CH_2 of C_6H_{11}), 25.67 (s, 1C, CH_2 of C_6H_{11}), 33.10 (s, 2C, CH_2 of C_6H_{11}), 48.65 (s, 1C, CH of C_6H_{11}), 70.37 (s, 2C, CH of fc), 70.77 (s, 2C, CH of fc), 72.40 (d, $J_{PC} = 10$ Hz, 2C, CH of fc), 75.41 (d, $J_{PC} = 13$ Hz, 2C, CH of fc), 128.40 (d, $^3J_{PC} = 12$ Hz, 4C, CH_m of PPh_2), 131.54 (d, $^2J_{PC} = 10$ Hz, 2C, CH_o of PPh_2), 131.88 (d, $^4J_{PC} = 2$ Hz, 4C, CH_p of PPh_2), 133.07 (br d, $^1J_{PC} = 107$ Hz, 2C, C_{ipso} of PPh_2), 168.55 (s, 1C, C═O); signals due to C_{ipso}(fc) are probably obscured by the solvent. IR (neat): ν 3240 br s, 3077 m, 3057 m, 2931 s, 2853 s, 1639 s, 1544 s, 1437 m, 1318 m, 1188 s, 1163 s, 1119 s, 1029 m, 837 m, 821 m, 750 s, 723 s, 701 s, 568 s, 526 s, 505 s cm^{-1}. Anal. Calc. for $C_{29}H_{30}PFeO_2N$ (511.4): C 68.11, H 5.91, N 2.74%. Found: C 68.32, H 6.02, N 2.53%.

4.3. Preparation of 1′-(diphenylphosphino)-1-(N-phenylcarbamoyl) ferrocene (**3**)

Phosphine-amide **3** was prepared similarly starting with **1** (450 mg, 1.0 mmol), *n*-butyllithium (0.5 mL 2.5 M in hexanes, 1.3 mmol) and phenylisocyanate (142 mg, 1.2 mmol). The workup and chromatographic isolation as described above (a second band was collected) gave phosphinoamide **3** as an orange foam (155 mg, 32%).

^1H NMR ($CDCl_3$): δ 4.12 (vq, $J' = 1.9$ Hz, 2H, fc), 4.27 (vt, $J' = 1.9$ Hz, 2H, fc), 4.48 (vt, $J' = 1.9$ Hz, 2H, fc), 4.68 (vt, $J' = 1.9$ Hz, 2H, fc), 7.09–7.64 (m, 15H, NPh and PPh_2), 7.75 (s, 1H, NH). $^{31}P\{^1H\}$ NMR ($CDCl_3$): δ −16.7 (s). $^{13}C\{^1H\}$ NMR ($CDCl_3$): δ 69.90 (s, 2C, CH of fc), 71.80 (s, 2C, CH of fc), 72.80 (d, $J_{PC} = 4$ Hz, 2C, CH of fc), 74.55 (d, $J_{PC} = 13$ Hz, 2C, CH of fc), 119.84 (s, 2C, CH_m of NPh), 123.97 (s, 1C CH_p of NPh), 128.38 (d, $^3J_{PC} = 6$ Hz, 4C, CH_m of PPh_2), 128.92 (s, 2C, CH_p of PPh_2), 129.01 (s, 2C CH_o of NPh), 133.47 (d, $^2J_{PC} = 20$ Hz, 4C, CH_o of PPh_2), 138.08 (d, $^1J_{PC} = 9$ Hz, 2C, C_{ipso} of PPh_2), 138.28 (s, 1C, C_{ipso} of NPh), 168.31 (s, 1C, C═O); signals due to ferrocene C_{ipso} are obscured by the solvent resonance. IR (Nujol): ν 3300 br s, 1650 s, 1637 s, 1597 s, 1528 s, 1499 s, 1434 s, 1320 s, 1272 m, 1161 w, 1141 w, 1028 m, 743 s, 695 s, 496 s, 450 m cm^{-1}. ESI ± MS: *m/z* 489 (M^+), 512 ($[M + Na]^+$); 488 ($[M - H]^-$). EI^+ MS: *m/z* (relative abundance) 491 (5), 490 (32), 489 (100, $M^{+\bullet}$), 488 (8), 487 (7), 462 (4), 412 (5, $[M - Ph]^+$), 397 (5, $[Ph_2PfcCO]^+$), 386 (8), 384 (3), 344 (6), 322 (10), 321 (32, $[C_5H_4PPhFeO]^+$), 305 (10, $[C_5H_4PPh_2Fe]^+$), 288 (11), 287 (5), 227 (4), 226 (8), 201 (5, $[Ph_2PO]^+$), 197 (3), 183 (5, $[PPh_2 - 2H]^+$), 171 (12), 170 (8), 141 (2). HR MS calc. for $C_{29}H_{24}{}^{56}FeNOP$ ($M^{+\bullet}$) 489.0945, found 489.0952. Anal. Calc. for $C_{29}H_{24}PFeON$ (489.3): C 71.18, H 4.94, N 2.86%. Found: C 70.86, H 4.91, N 2.76%.

4.4. Preparation of trans-dichloridobis[1′-(diphenylphosphino-κP)-1-(N-phenylcarbamoyl)ferrocene]palladium(II) (**5**)

Amide **3** (19.6 mg, 0.04 mmol) and $[PdCl_2(cod)]$ (5.7 mg, 0.02 mmol) were dissolved in chloroform (10 mL) to give a red solution. The mixture was stirred for 2.5 h and layered with diethyl ether. During crystallisation at 4 °C over several days, the mixture deposited a solid, which was filtered off, washed with diethyl ether and dried under vacuum to afford **5**·0.35$CHCl_3$ as an orange-brown microcrystalline solid (16 mg, 69%).

^1H NMR ($CDCl_3$): δ 4.53 (br s, 2H, fc), 4.60 (br s, 2H, fc), 4.64 (br s, 2H, fc), 5.04 (br s, 2H, fc), 7.04–7.69 (m, 15H, NPh and PPh_2), 7.85 (s, 1H, NH). $^{31}P\{^1H\}$ NMR ($CDCl_3$): δ +16.3 (s). IR (Nujol): ν 3420 br m, 1678 s, 1595 m, 1529 s, 1496 w, 1314 s, 1264 w, 1162 m, 1140 w, 1098 m, 839 w, 745 s, 689 s, 516 m, 497 m, 473 m cm^{-1}. ESI+ MS: *m/z* 1177/1179 ($[M + Na]^+$), 1119/1120 ($[M - Cl]^+$), 1041/1043 ([PdCl(**3**)(**3** − H) + Na]$^+$). Anal. Calc. for $C_{58}H_{48}P_2Fe_2O_2N_2PdCl_2 \cdot 0.35CHCl_3$ (1197.7): C 58.51, H 4.07, N 2.34%. Found: C 58.44, H 4.29, N 2.18%.

4.5. Preparation of trans-dichloridobis[1′-(diphenylphosphino-κP)-1-(N-phenylcarbamoyl)ferrocene]platinum(II) (**6**)

Aqueous solution of $Na_2[PtCl_4]$ (7.7 mg, 0.02 mmol in 0.5 mL of water) was added to a solution of amide **3** (20 mg, 0.04 mmol) in glacial acetic acid (10 mL), causing immediate separation of an orange precipitate. The mixture was stirred for 1 h and then heated until the solids dissolved. The mixture was filtered (PTFE syringe filter 0.45 μm) while hot and the filtrate was allowed to crystallise by slow cooling to 4 °C. The separated crystalline product was filtered off, washed sequentially with 50% aqueous acetic acid and water, and dried under vacuum to afford the solvate **6**·3AcOH as an orange crystalline solid (20 mg, 40%).

^1H NMR ($CDCl_3$): δ 4.52 (vt, $J' \approx 1.8$ Hz, 2H, fc), 4.61 (vt, $J' \approx 1.8$ Hz, 2H, fc), 4.66 (vt, $J' \approx 1.8$ Hz, 2H, fc), 5.04 (vt, $J' \approx 1.8$ Hz, 2H, fc), 7.05–7.70 (m, 15H, NPh and PPh_2), 7.73 (s, 1H, NH). $^{31}P\{^1H\}$ NMR ($CDCl_3$): δ +11.1 (s with ^{195}Pt satellites, $^1J_{PtP} = 2605$ Hz). IR (Nujol): ν 3330 br s, 1713 s, 1632 s, 1600 s, 1544 s, 1500 s, 1377 s, 1325 m, 1275 m, 1036 w, 752 m, 694 w, 527 w cm^{-1}. ESI ± MS: *m/z* 1267 ($[M + Na]^+$); 1243 ($[M - H]^-$). Anal. Calc. for $C_{58}H_{48}P_2Fe_2O_2N_2PtCl_2 \cdot 3AcOH$ (1424.8): C 53.95, H 4.24, N 1.97%. Found: C 53.71, H 4.14, N 1.96%.

4.6. Preparation of cis-dichloridobis[1′-(diphenylphosphino-κP)-1-(N-phenylcarbamoyl)ferrocene]platinum(II) (**7**)

Amide **3** (20 mg, 0.04 mmol) and $[PtCl_2(cod)]$ (7.5 mg, 0.02 mmol) were dissolved in chloroform (10 mL). The mixture was stirred for 2 h and then layered with diethyl ether. Crystallisation at 4 °C over several days afforded a crystalline solid which was filtered off, washed with diethyl ether, and dried under vacuum to give **7**·0.5$CHCl_3$ (orange microcrystalline solid; 16.5 mg, 33%).

^1H NMR ($CDCl_3$): δ 3.75 (vt, $J' = 1.9$ Hz, 2H, fc), 4.07 (br s, 2H, fc), 4.26 (br s, 2H, fc), 4.66 (vt, $J' = 1.9$ Hz, 2H, fc), 7.06–7.76 (m, 15H, NPh and PPh_2), 9.39 (s, 1H, NH). $^{31}P\{^1H\}$ NMR ($CDCl_3$): δ +9.4 (s with ^{195}Pt satellites, $^1J_{PtP} = 3785$ Hz). IR (Nujol): ν 3300 br m, 1670 s, 1641 s, 1597 s, 1534 s, 1316 s, 1269 m, 1164 m, 834 w, 755 m, 690 s, 489 s cm^{-1}. ESI ± MS: *m/z* 1209 ($[M - Cl]^+$), 1173 ($[M - 2Cl]^+$); 1243 ($[M - H]^-$). Anal. Calc. for $C_{58}H_{48}P_2Fe_2O_2N_2PtCl_2 \cdot 0.5CHCl_3$ (1304.3): C 53.87, H 3.75, N 2.15. Found: C 53.60, H 3.87, N 2.10%.

4.7. Preparation of [SP-4-4]-chlorido{[(2-dimethylamino-κN) methyl]phenyl-κC^1}-[1′-(diphenylphosphino-κP)-1-(N-phenylcarbamoyl)ferrocene]palladium(II) (**8**)

Di-μ-chloridobis{[(2-dimethylamino-κ*N*)methyl]phenyl-κC^1} dipalladium(II) (11 mg, 0.02 mmol) and amide **3** (20 mg, 0.04 mmol) were dissolved in dry chloroform (10 mL). The resultant solution was stirred for 2 h, partially evaporated under vacuum, and precipitated with pentane (15 mL). The mixture was cooled to −18 °C overnight, and the precipitate was filtered off, washed with pentane and dried under vacuum to give complex **8**·0.7$CHCl_3$ as an orange solid (19 mg, 63%).

^{1}H NMR ($CDCl_3$): δ 2.86 (d, $^4J_{PH}$ = 2.7 Hz, 6H, NMe_2), 4.14 (d, $^4J_{PH}$ = 2.4 Hz, 2H, NCH_2), 4.46–4.50 (m, 4H, fc), 4.67 (vt, J' = 1.9 Hz, 2H, fc), 5.21 (vt, J' = 1.9 Hz, 2H, fc), 6.24 (ddd, J = 7.8, 6.5, 1.2 Hz, 1H, C_6H_4), 6.35 (td, J = 7.5, 1.4 Hz, 1H, C_6H_4), 6.81 (td, J = 7.4, 1.1 Hz, 1H, C_6H_4), 7.00 (dd, J = 7.4, 1.6 Hz, 1H, C_6H_4) 7.06–7.79 (m, 15H, NPh and PPh_2), 8.59 (s, 1H, NH). ^{31}P{^{1}H} NMR ($CDCl_3$): δ +32.9 (s). IR (Nujol): ν 3300 br s, 1666 s, 1596 s, 1529 s, 1315 s, 1164 m, 1099 m, 1028 m, 844 m, 693 s cm^{-1}. ESI ± MS: *m*/*z* 729 ([M − Cl]$^+$); 763 ([M − H]$^-$), 488 ([**3** − H]$^-$). Anal. Calc. for $C_{38}H_{36}PFeON_2PdCl\cdot 0.7CHCl_3$ (848.9): C 54.75, H 4.36, N 3.30. Found: C 54.74, H 4.45, N 3.24%.

4.8. Preparation of [SP-4-3]-{[(2-dimethylamino-κN)methyl] phenyl-κC^1}-[1′-(diphenylphosphino-κP)-1-(N-phenylcarbamoyl-κO)ferrocene]palladium(II) hexafluoroantimonate (**9**)

Di-μ-chloridobis{[(2-dimethylamino-κ*N*)methyl]phenyl-κC^1} dipalladium(II) (27.5 mg, 0.05 mmol) and amide **3** (20 mg, 0.04 mmol) were dissolved in dry dichloromethane (3 mL) and the resulting solution was stirred at room temperature for 15 min. Then, a solution of Ag[SbF_6] (35 mg, 0.10 mmol) in dry tetrahydrofuran (1 mL) was added, causing separation of an off-white precipitate (AgCl). The mixture was stirred for another 15 min, filtered (0.45 μm PTFE syringe filter), and the filtrate was layered with diethyl ether. Subsequent crystallisation by liquid-phase diffusion at 4 °C afforded orange-brown crystalline solid, which was isolated by suction, washed with diethyl ether and dried under vacuum. Yield: 83 mg (86%), rusty orange crystals.

^{1}H NMR ($(CD_3)_2SO$): δ 2.68 (d, $^4J_{PH}$ = 2.7 Hz, 6H, NMe_2), 3.97 (vq, J = 2.0 Hz, 2H, fc), 4.17 (unresolved d, 2H, NCH_2), 4.47 (vt, J = 2.0 Hz, 2H, fc), 4.57 (m, 2H, fc), 5.15 (vt, J = 2.0 Hz, 2H, fc), 6.28 (ddd, J = 7.6, 6.2, 1.0 Hz, 1H, C_6H_4), 6.47 (td, J = 7.6, 1.6 Hz, 1H, C_6H_4), 6.90 (td, J = 7.4, 1.0 Hz, 1H, C_6H_4), 7.07 (dd, J = 7.4, 1.6 Hz, 1H, C_6H_4), 7.09–7.75 (m, 15H, NPh and PPh_2), 9.70 (s, 1H, NH). ^{31}P{^{1}H} NMR ($(CD_3)_2SO$): δ +31.0 (s). IR (Nujol): ν 3394 m, 1611 s, 1594 s, 1580 m, 1337 s, 1282 m, 1240 w, 1167 m, 1096 m, 1038 w, 1027 w, 1019 w, 992 w, 973 w, 863 w, 876 m, 836 w, 827 w, 761 s, 752 w, 741 m, 695 s, 655 s, 639 s, 533 m, 522 m, 515 m, 507 s, 474 m cm^{-1}. ESI ± MS: *m*/*z* 729 ([(L^{NC})Pd(**3**)]$^+$); 488 ([**3** − H]$^-$), 235/237 ([SbF_6]$^-$). Anal. Calc. for $C_{38}H_{36}F_6FeN_2OPPdSb$ (965.7): C 47.26, H 3.76, N 2.90%. Found: C 46.91, H 3.94, N 2.78%.

4.9. X-ray crystallography

Single crystals suitable for diffraction analysis were selected directly from the reaction batch (**9**: orange-brown prism, 0.19 × 0.30 × 0.44 mm^3), or grown by crystallisation from ethyl acetate/hexane (**4**: orange prism, 0.28 × 0.30 × 0.80 mm^3) or chloroform/diethyl ether (**5**·2Et_2O: red block, 0.25 × 0.55 × 0.60 mm^3). Full-set diffraction data ($\pm h \pm k \pm l$, $2\theta \leq 55°$, data completeness ≥98.5%) were collected with a Nonius KappaCCD diffractometer equipped with a Cryostream Cooler (Oxford Cryosystems) using graphite monochromatised MoKα radiation (λ = 0.71073 Å) and were corrected for absorption using the methods incorporated in the diffractometer software.

The structures were solved by direct methods (SIR97, Ref. [22]) and refined by full-matrix least-squares based on F^2 (SHELXL97, Ref. [23]). Non-hydrogen atoms were refined with anisotropic displacement parameters. Amide hydrogens (H1N) were identified on the difference electron density maps and refined as riding atoms with unconstrained isotropic displacement parameters. All other hydrogen atoms were included in their calculated positions and treated as riding atoms with U_{iso}(H) assigned to a multiple of U_{eq} of their bonding carbon atom. The solvent molecules in the structure of **5**·2Et_2O were found to be severely disordered in structural voids defined by the bulky complex molecules of the complex. Their contribution to the overall diffraction intensity was modelled by SQUEEZE routine as incorporated in PLATON program [24]. Within the 714 Å^3 of void space per the unit cell, a total of 145 electrons were calculated, compared to the 168 electrons expected for four molecules of diethyl ether.

Relevant crystallographic data are summarised in Table 5. Geometric parameters and structural drawings were obtained with a recent version of the PLATON program [24]. All numerical values are rounded with respect to their estimated standard deviations (esd's) given with one decimal; parameters involving fixed hydrogen atoms are given without esd's.

Acknowledgements

This work is a part of the long-term research project of Faculty of Science, Charles University in Prague supported by the Ministry of Education, Youth and Sports of the Czech Republic (project no. MSM0021620857).

Appendix A. Supplementary material

CCDC 773800–773802 contain the supplementary crystallographic data for this paper. These data can be obtained free of charge from The Cambridge Crystallographic Data Centre via www.ccdc.cam.ac.uk/data_request/cif.

References

[1] (a) L. Meca, D. Dvořák, J. Ludvík, I. Císařová, P. Štěpnička, Organometallics 23 (2004) 2541;
(b) P. Štěpnička, J. Schulz, I. Císařová, K. Fejfarová, Collect. Czech. Chem. Commun. 72 (2007) 453;
(c) M. Lamač, I. Císařová, P. Štěpnička, Eur. J. Inorg. Chem. (2007) 2274;
(d) J. Kühnert, M. Dušek, J. Demel, H. Lang, P. Štěpnička, Dalton Trans. (2007) 2802;
(e) M. Lamač, J. Tauchman, I. Císařová, P. Štěpnička, Organometallics 26 (2007) 5042;
(f) J. Kühnert, M. Lamač, J. Demel, A. Nicolai, H. Lang, P. Štěpnička, J. Mol. Catal. A: Chem. 285 (2008) 41;
(g) J. Kühnert, I. Císařová, M. Lamač, P. Štěpnička, Dalton Trans. (2008) 2454;
(h) J. Tauchman, I. Císařová, P. Štěpnička, Organometallics 28 (2009) 3288;
(i) J. Schulz, I. Císařová, P. Štěpnička, J. Organomet. Chem. 694 (2009) 2519;
(j) P. Štěpnička, M. Krupa, M. Lamač, I. Císařová, J. Organomet. Chem. 694 (2009) 2987;
(k) M. Lamač, I. Císařová, P. Štěpnička, New J. Chem. 33 (2009) 1549;
(l) M. Lamač, J. Tauchman, S. Dietrich, I. Císařová, H. Lang, P. Štěpnička, Appl. Organomet. Chem. 24 (2010) 326.
[2] For examples from other laboratories, see: (a) W. Zhang, T. Shimanuki, T. Kida, Y. Nakatsuji, I. Ikeda, J. Org. Chem. 64 (1999) 6247;
(b) J.M. Longmire, B. Wang, X. Zhang, J. Am. Chem. Soc. 124 (2002) 13400;
(c) S.-L. You, X.-L. Hou, L.-X. Dai, J. Organomet. Chem. 637–639 (2001) 762;
(d) J.M. Longmire, B. Wang, X. Zhang, Tetrahedron Lett. 41 (2000) 5435;
(e) S.-L. You, X.-L. Hou, L.-X. Dai, B.-X. Cao, J. Sun, Chem. Commun. (2000) 1933;
(f) M. Tsukazaki, M. Tinkl, A. Roglans, B.J. Chapell, N.J. Taylor, V. Snieckus, J. Am. Chem. Soc. 118 (1996) 685;
(g) H. Jendralla, E. Paulus, Synlett (1997) 471.
[3] This method is widely used for conjugation of biomolecules with ferrocenecarboxylic acids: (a) N. Metzler-Nolte, M. Salmain, in: P. Štěpnička (Ed.), The

Bioorganometallic Chemistry of Ferrocene in Ferrocenes: Ligands, Materials and Biomolecules, Wiley, Chichester, 2008 (chapter 13) pp. 499–639;
(b) H.-B. Kraatz, J. Inorg. Organomet. Polym. Mater. 15 (2005) 83;
(c) For examples of phosphinocarboxamides prepared by this approach, see Refs. [1a–l].
[4] W. Zhang, Y. Yoneda, T. Kida, Y. Nakatsuji, I. Ikeda, Tetrahedron: Asymmetry 9 (1998) 3371.
[5] N. Weliky, E.S. Gould, J. Am. Chem. Soc. 79 (1957) 2742.
[6] (a) Grignard reagents were originally used: E.E. Blaise C.R. Acad. Sci. 132 (1901) 38. For other early examples of the preparation of carboxamides from organolithium or Grignard reagents and isocyanates, see:
(b) U. Schöllkopf, Methoden der organischen Chemie (Houben-Weyl), fourth ed., vol. XIII/1, Thieme, Stuttgart, 1970, p. 190;
(c) K. Nützel, Methoden der organischen Chemie (Houben-Weyl), fourth ed., vol. XIII/2a, Thieme, Stuttgart, 1973, p. 393.
[7] (a) D.W. Slocum, B.W. Rockett, C.R. Hauser, J. Am. Chem. Soc. 87 (1965) 1241;
(b) D.W. Slocum, C.A. Jennings, T.R. Engelmann, B.W. Rockett, C.R. Hauser, J. Org. Chem. 36 (1971) 377.
[8] M. Oberhoff, L. Duda, J. Karl, R. Mohr, G. Erker, R. Fröhlich, M. Grehl, Organometallics 15 (1996) 4005.
[9] (a) I.R. Butler, R.L. Davies, Synthesis (1996) 1350;
(b) P. Štěpnička, in: P. Štěpnička (Ed.), 1′-Functionalised Ferrocene Phosphines: Synthesis, Coordination Chemistry and Catalytic Applications in Ferrocenes: Ligands, Materials and Biomolecules, Wiley, Chichester, 2008 (chapter 5) pp. 177–204 and references cited therein.
[10] J. Podlaha, P. Štěpnička, J. Ludvík, I. Císařová, Organometallics 15 (1996) 543.
[11] H.-O. Kalinowski, S. Berger, S. Braun, ^{13}C-NMR-Spektroskopie. Thieme, Stuttgart, 1984, (chapter 4).
[12] In the case of amide **2**, this ion falls into the isotopic cluster due to a highly strong fragment at *m*/*z* 400.
[13] M. Polášek, P. Štěpnička, J. Mass Spectrom. 33 (1998) 739.
[14] D. Cremer, J.A. Pople, J. Am. Chem. Soc. 97 (1975) 1354.
[15] (a) F.R. Hartley, The Chemistry of Platinum and Palladium. Applied Science, London, 1973, (chapter 7) pp. 136–140 and references cited therein;
(b) P.S. Pregosin, R.W. Kunz, in: P. Diehl, E. Fluck, R. Kosfeld (Eds.), NMR-Basic Principles and Progress: ^{31}P and ^{13}C NMR of Transition Metal Phosphine Complexes, vol. 16, Springer, Berlin, 1979, pp. 47–56.
[16] P. Štěpnička, J. Podlaha, R. Gyepes, M. Polášek, J. Organomet. Chem. 552 (1998) 293.
[17] For NMR data of (L^{NC})Pd-complexes with phosphinoferrocene ligands, see: (a) J.-M. Ma, Y. Yamamoto, Inorg. Chim. Acta 299 (2000) 164;
(b) P. Štěpnička, I. Císařová, Organometallics 22 (2003) 1728;
(c) P. Štěpnička, Inorg. Chem. Commun. 7 (2004) 426;
(d) P. Štěpnička, M. Lamač, I. Císařová, Polyhedron 23 (2004) 921;
(e) P. Štěpnička, I. Císařová, Inorg. Chem. 45 (2006) 8785;
(f) P.I. ŠtěpničkaCísařová, Collect. Czech. Chem. Commun. 71 (2006) 215 See also Refs. [1h,j].
[18] K. Nakamoto, Infrared and Raman Spectra of Inorganic and Coordination Compounds, Part A: Theory and Applications in Inorganic Chemistry, fifth ed. Wiley, New York, 1997, part A, sect. II (chapter II-8) p. 214.
[19] Composition of the crystallised material and the 'bulk' product differ owing to a different crystallisation procedure.
[20] D. Drew, J.R. Doyle, Inorg. Synth. 13 (1972) 47.
[21] A.C. Cope, E.C. Friedrich, J. Am. Chem. Soc. 90 (1968) 909.
[22] A. Altomare, M.C. Burla, M. Camalli, G.L. Cascarano, C. Giacovazzo, A. Guagliardi, A.G.G. Moliterni, G. Polidori, R. Spagna, J. Appl. Crystallogr. 32 (1999) 115.
[23] G.M. Sheldrick, SHELXL97. Program for Crystal Structure Refinement from Diffraction Data. University of Göttingen, Göttingen, 1997.
[24] A.L. Spek, J. Appl. Crystallogr. 36 (2003) 7.